Surface Reactivity from Electrochemical Lithography: Illustration in the Steady-State Reductive Etching of Perfluorinated Surfaces.

Hassan Hazimeh, Sandra Nunige, Renaud Cornut, Christine Lefrou, Catherine Combellas, Frédéric Kanoufi

Supporting Information

Experimental Section

Materials

Glass substrates were 1.1 mm thick microscope slides, Si/SiO_2 substrates were 1x1 cm^2 plaques (from 2 inches wafers, ACS). ITO was provided by Saint-Gobain Recherche (Aubervilliers, France). Glass substrates were cleaned with a freshly prepared piranha solution (70:30 v/v, concentrated H_2SO_4 /aqueous H_2O_2 (35%)) at 150 °C for 30 min. ITO was cleaned in an alkaline piranha solution (5:1:1 v/v/v, H_2O:H_2O_2 (30%):NH_4OH (25%)) at 70°C for 1 h. The substrates were then rinsed with pure water (Millipore, resistivity ≥ 18.2 MΩ cm), cleaned by ultrasonication in water for 1 min, and dried under nitrogen. Silanization was conducted in the same way for the three kinds of substrates in order to give the fluorinated SAMs: in the gas phase, the substrates were placed in a sealed cell in the presence of an open flask of 1H,1H,2H,2H-perfluorodecyltrichlorosilane ($CF_3(CF_2)_7(CH_2)_2SiCl_3$, 97%), heated at 110 °C for 2 h. All chemicals were from Aldrich and used as received.

Electrochemical characterizations.

Cyclic voltammetric experiments were performed with a classical three-electrode setup with a 250 µm diameter Pt wire counter-electrode and a 250 µm Ag/AgCl wire (pseudo-reference). SECM

experiments were performed with a home-made SECM described previously and equipped with a CH660 potentiostat (CH Instruments, Austin, Tx, USA).[1]

The tips used were Pt wires embedded in glass (RG = 5 for a = 12.5 and 25 μm and RG = 12 for a = 5 μm, a = active radius and RG = ratio of insulating sheath to metal radii). To measure a steady-state current, the tip was approached to the (unbiased) substrate at a constant approach speed of 1 μm/s. The tip current, i_T, was recorded as a function of the tip displacement (tip/substrate distance, d) and converted into an approach curve, $I_T = f(d/a)$ by normalization of i_T by its value at infinite d, $i_{T,inf}$. In the feedback mode, typically, the microelectrode-substrate positioning was obtained from the experimental approach curve of ferrocyanide onto the surface.

Redox catalysis experiments were carried out for each redox mediator with at least : 4 scan rates, v, 2 values of the excess factor, γ, (γ, is the ratio of substrate over mediator concentration) and 3 mediator concentrations. The homogeneous rates constants given were the averages of at least 24 values per redox mediator. The redox catalysis experiments were performed with 3 mm diameter glassy carbon electrodes as described elsewhere.[2] Briefly, the experiments consist of recording the cyclic voltammogram of the redox mediator reduction and comparing the peak current in the absence, i_{p0}, and in the presence, i_p, of the investigated perfluoroalkane. The peak current enhancement, i_p/i_{p0} is then used to extract the kinetics of the homogeneous electron transfer, k_{hom}, between the electrogenerated reduced form of the redox mediator and the perfluoroalkane. The rate constant determination relies on the theoretical variation $i_p/i_{p0} = f(k_{hom}, [M], \gamma, v)$ obtained from digital simulation (DIGISIM®, BioAnalytical System). As the reduction corresponds to the complete defluorination of the perfluoroalkane by the injection of 2 electrons per broken C-F bond (see section 2), the excess factor used to simulate the experimental variation of i_p/i_{p0} is $2n_{CF}\gamma$.

[1] Combellas, C.; Ghilane, J.; Kanoufi, F.; Mazouzi, D. *J. Phys. Chem. B* **2004**, *108*, 6391.
[2] Combellas, C.; Kanoufi, F.; Thiébault A. *J. Phys. Chem. B* **2003**, *107*, 10894-10905.

Patterning.

Patterning of the fluorinated SAM was performed with the same SECM apparatus. Reduction of the fluorinated layer was achieved in a solution of DMF containing NBu_4BF_4 and a redox mediator (tri-*p*-tolylphosphine, TPP), by applying a reductive potential of -2.85 V/Ag/AgCl to the tip. The whole device was kept under nitrogen in a polyethylene glovebag during the experiment. The pattern dimensions were measured as reported elsewhere[3] from the preferred condensation of water vapor onto the patterned surfaces.

COMSOL modelizations.

The cell chosen for the modelization is described in Scheme SI1, the far-field boundaries are given by Rs = 1000 and Zs = 1000.

The model discussed in the Theoretical Section corresponds to stationary calculation of the dimensionless concentration distribution of the etchant (Red in Scheme 1), c, from diffusion equation resolution (stationary form of S1 - $\frac{\partial C}{\partial \tau} = 0$ with τ and t the dimensionless an real time respectively, $t = \tau a^2/D$) in the whole cell and further estimate of the etchant concentration profile at the substrate surface. The consideration of etchant lifetime, with dimensionless decay rate $\lambda_c = k_c a^2/D$, needs the consideration of second species, namely P in Scheme 1, of dimensionless concentration p whose variation is given by (S2). It is not necessary to compute the concentration of the mediator in its initial form (Ox in Scheme 1) since it is directly deduced from $[Ox] = C_0 (1 - c - p)$.

$$\frac{\partial c}{\partial \tau} = \frac{\partial^2 c}{\partial Z^2} + \frac{\partial^2 c}{\partial R^2} + \frac{1}{R}\frac{\partial c}{\partial R} - \lambda_c c \qquad \text{(S1)}$$

$$\frac{\partial p}{\partial \tau} = \frac{\partial^2 p}{\partial Z^2} + \frac{\partial^2 p}{\partial R^2} + \frac{1}{R}\frac{\partial p}{\partial R} + \lambda_c c \qquad \text{(S2)}$$

[3] Ktari, N.; Nunige, S.; Azioune, A.; Piel, M.; Connan, C.; Kanoufi, F.; Combellas C. *Chem. Mater.* **2010**, *22*, 5725.

For the transient etching of ITO surface, a transient resolution was used ($\frac{\partial C}{\partial \tau} \neq 0$ in S1 and S2). The transient transformation of the surface is obtained by considering two new boundaries at the substrate instead of the dC/dN=0 condition. The first one corresponds to the layer surface transformation during the etching (S3) at the dimensionless rate $\lambda_{etch}=k_{etch}C^0a^2/D$. θ_{CF} represents the surface coverage of the unetched layer. The second one corresponds to the feedback increase observation and originates from the facilitated ET, at the dimensionless rate $\lambda_{S,CFred}=k_{S,CFred}a/D$, at the etched fluorinated surface (eq (11) in the text; expressed in its dimensionless form in (S4)).

$$\frac{\partial \theta_{CF}}{\partial \tau} = -\lambda_{etch}\ \theta_{CF}\ c \qquad \text{(S3)}$$

$$-\frac{\partial c}{\partial N} = -\lambda_{S,CFred} S\ (1-\theta_{CF})\ c \qquad \text{(S4)}$$

The description of the problem in COMSOL® was achieved by considering the substrate as a new 1D-axi-symmetric geometric cell where the variable θ_{CF} is defined. The boundary relationship between θ_{CF} and the solution etchant concentration c (S3 and 4) are satisfied by using the solution concentrations (c and p) and the surface coverage θ_{CF} variables respectively extruded from 2D to 1D geometries or from 1D to 2D geometries. Typically, the solution concentrations in the 2D geometry are extruded in the 1D geometry into the extruded variables defined by c_{ex} and p_{ex}. Similarly, the surface coverage defined in the 1D cell is extruded into the 2D geometric cell in the extruded variable θ_{ex}. These boundaries (S3) and (S4) are expressed accordingly in COMSOL® by (S5) and (S6), which apply at the substrate, respectively in the 2D or 1D geometries:

$$\frac{\partial \theta_{CF}}{\partial \tau} = -\lambda_{etch}\ \theta_{CF}\ c_{ex,(R,Z=0} \qquad \text{(S5)}$$

$$-\frac{\partial c}{\partial N} = -\lambda_{S,CFred}\ (1-\theta_{ex})\ c_{R,Z=0} \qquad \text{(S6)}$$

The transient resolution of (S1 to S4) yields the evolution of the species concentrations and surface coverage with the dimensionless time, τ. The fit of the experimental data consists of comparing the experimental and theoretical tip current variations. It is evaluated by computing the function reacf. This function has been especially implemented by the software developers to have a more accurate evaluation for a flux. The tip current is then obtained from the flux.

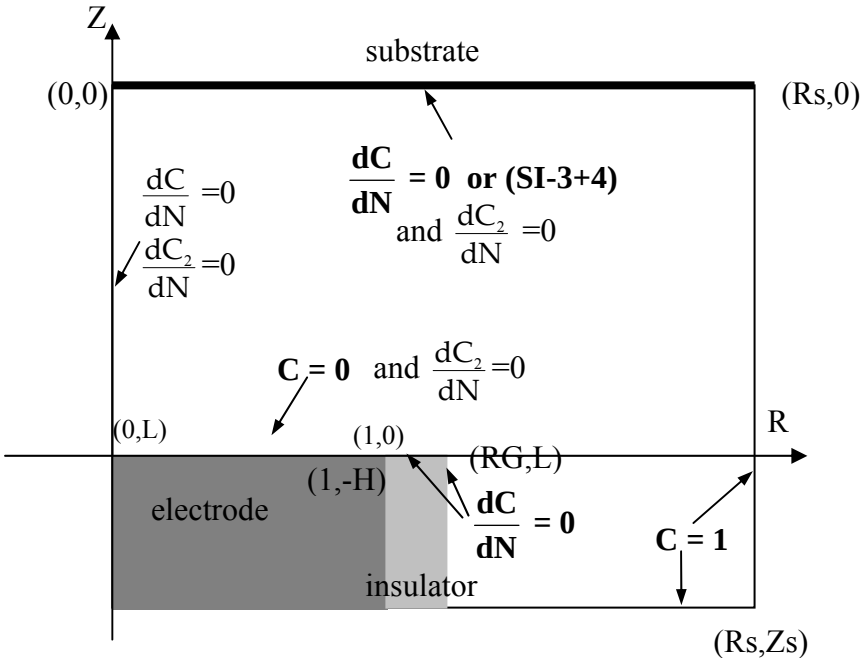

Figure SI-1: Scheme of the electrochemical cell for SECM modelization of etchant electrogeneration at a tip, and boundary conditions.

Influence of the tip-substrate distance on the pattern dimensions.

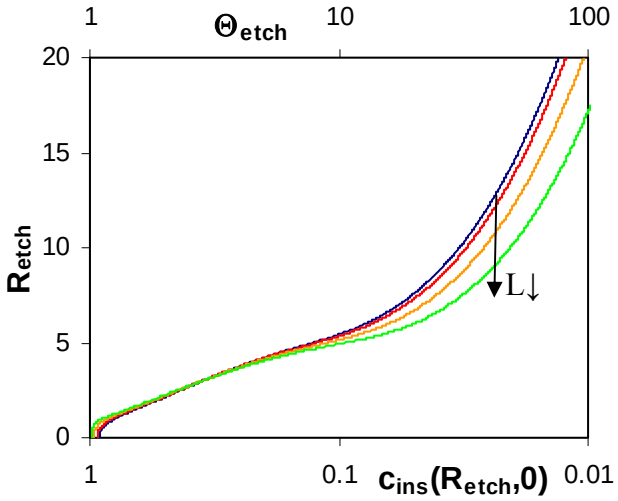

Figure SI-2. Influence on the theoretical evolution of the pattern dimension of the dimensionless tip-substrate separation distance L=d/*a* at fixed RG=5, from top to bottom L = 0.68, 0.62, 0.5, 0.37.

The influence of the tip-substrate separation distance is presented in Figure SI-2. Interestingly, for etching times lower than 10 times the characteristic etching lifetime ($\Theta_{etch} < 10$), the pattern dimension is independent of L when the etching is confined under the electrode insulating sheath ($R_{etch} < RG$). This comes from the special shape of isoconcentrations that are majoritarily perpendicular to the substrate. Analytical resolution of negative feedback situation in the small probe substrate distance situation[1] leads to an expression of the concentration profile underneath the insulating sheet that is independent of L : $C_{ins}(R_{etch}) \approx 1-\ln(R_{etch}/RG)$. The influence of L is markedly observed at longer times when the pattern dimension exceeds the electrode insulating sheath ($R_{etch} > RG$) and the larger L, the larger the pattern for the same etching time. This simply reflects that the etchant transport outside the tip insulating sheath is very small and governed by the hindered transport within the thin layer cell defined by the tip-substrate geometry: the shorter L, the smaller the etchant concentration at the exit of

this thin layer cell (at RG), then the easier the etchant is diluted in the bulk at the substrate surface for R>RG.

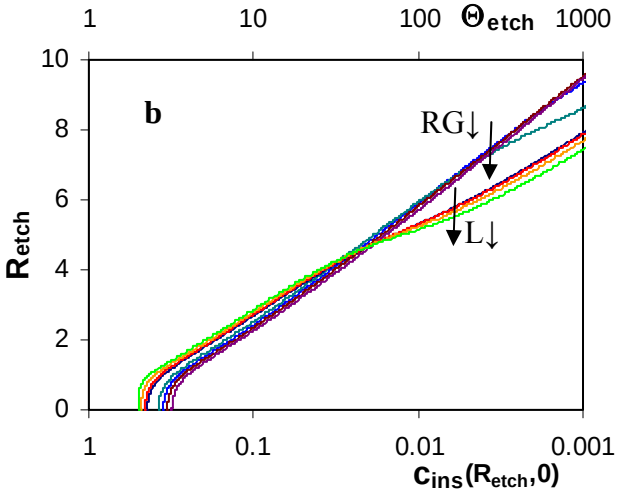

Figure SI-3. Influence on the theoretical evolution of the pattern dimension of the dimensionless tip-substrate separation distance L=d/*a* and RG values at fixed λ_c = 0.3 and with variable RG and L, from top to bottom: L=0.68 and RG= 15, 12, 10, 8; then RG=5 and L= 0.68, 0.62, 0.5, 0.37.

For a given value of λ_c, Figure SI-3 shows that chemically unstable etchants confine the surface transformation to patterns comparable to the tip dimension without significant importance of L or, to a lesser extent, of RG, at least as long as the patterns are smaller than RG. Finally, for a given L or RG, under the conditions of unstable etchants, the pattern dimension, R_{etch}, varies linearly with the logarithm of the etching time, log(t), and the more unstable the etchant (the higher λ_c), the smaller the slope of this variation.

Cyclic voltammetry analysis of ET through SAMs on ITO

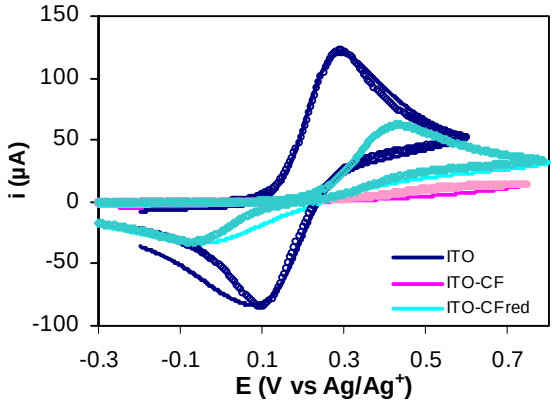

Fig SI-4. Cyclic voltammetry of $Fe(CN)_6^{4-}$ oxidation at ITO electrodes: — bare (ITO); — silanized with a perfluorinated silane (ITO-CF); — after silanization, etched by local SECM reduction on a 2x2 mm^2 square (ITO-CFred).

Figure SI-4 shows the experimental CV of ferrocyanide, $Fe(CN)_6^{4-}$, oxidation on surfaces of (—) a naked ITO or (—) an ITO covered by a perfluorinated SAM that is further (—) locally patterned by SECM. The silanization of the surface clearly blocks the electron transfer (ET) kinetics, as the ferrocyanide oxidation is displaced to higher potentials and occurs with much lower currents. The rates of the ET at the virgin or covered ITO surfaces are deduced from the digital simulation of the voltammograms according to Amatore's model of ET at blocked electrodes or from convolution analysis.[2,3] Indeed, for a quasi-reversible process, the variation of the electron transfer rate, k, with the potential, E, is given from the current, i(E), by:

$$k(E) \approx \frac{i(E)\sqrt{D}}{I_{\lim} - I(E)(1+\exp(-nF/RT(E-E^0)))} \qquad (9)$$

where I_{lim} is the diffusion limiting current of the sigmoidal convoluted current, *I(E)*, and *D* the probe diffusion coefficient ($D = 7x10^{-6}$ cm^2/s). The extrapolation of log k(E) to $E=E^0$ leads to k^0_{CV}. Both

analyses of the CVs gave similar values for the apparent standard heterogeneous ET at the naked, $k^0_{CV,ITO}$ = 1.5x10^{-3} cm s^{-1}, and covered, $k^0_{CV,CF}$= 1.0x10^{-5} cm s^{-1}, ITO electrodes.

The value of the ET through the perfluorinated silane SAM is lower or comparable to that observed through layers of alkyl chains of equivalent length bound to hydrogenated p-Si electrodes (8-10x10^{-4} cm s^{-1} for Si-$C_{10}H_{21}$).[4] This suggests that i) the silanization procedure with perfluoroalkyl chains gives comparable to higher surface coverage than those obtained from Si-C bond formation by reaction of hydrogenated Si with alkenes and ii) the silanization of Si/SiO_2 surfaces produces dense layers of chains, which are almost perpendicular to the surface. The low value of the ET attenuation (β=0.025 Å^{-1})[5] for electron tunneling through the Si-C monolayers also accounts for the formation of less dense or more tilted chains on hydrogenated Si. Still, even if the perfluorinated silane layer formed on the ITO electrode is more blocking than the Si-C layers, the ET to the covered ITO is mainly performed by defect sites of the perfluorinated silane layer.

The same CV analysis with ferrocyanide as the redox probe was performed on (wholly or locally) reduced perfluorinated layers assembled on ITO electrodes. After reduction of the perfluorinated SAM, even though the $Fe(CN)_6^{4-}$ oxidation is enhanced and recovers a diffusive shape (Figure 4A —), the etched layer still blocks the ET compared to the bare ITO electrode. From the CV analysis according to (10), the ET rate constant through this etched layer, $k^0_{CV,CFred}$ = 8x10^{-5} cm s^{-1}, is 8 times higher than on the perfluorinated layer but is still 18 times lower than on bare ITO.

---

[1] a) Cornut, R.; Lefrou, C. *J. Electroanal. Chem.* **2007**, *608*, 59. b) Lefrou, C.; Cornut, R. *Chem. Phys. Chem.* **2010**, *11*, 547.
[2] Matrab, T.; Hauquier, F.; Combellas, C.; Kanoufi, F. *ChemPhysChem* **2010**, *11*, 670.
[3] a) Amatore, C.; Savéant, J.-M.; Tessier, D. *J. Electroanal. Chem.* **1983**, *147*, 39. b) Bard, A. J.; Faulkner, L. R., Eds. In *Electrochemical Methods, Fundamentals and Application*, 2nd Ed., Wiley: New-York, 2001, p. 250.
[4] Hauquier, F.; Ghilane, J.; Fabre, B.; Hapiot, P. *J. Am. Chem. Soc.* **2008**, *130*, 2748.
[5] The slope of the variations of ln k with the number of C of the alkyl chain given in Fig 7 and Table 1 of ref 4 yields a value of β = 0.25 (instead of 1 as quoted in the text).